Chemical Engineering Journal 160 (2010) 729–737

Contents lists available at ScienceDirect

Chemical Engineering Journal

journal homepage: www.elsevier.com/locate/cej

Gas holdup, bubble behavior and mass transfer in a 5 m high internal-loop airlift reactor with non-Newtonian fluid

Zhonghuo Deng, Tiefeng Wang*, Nian Zhang, Zhanwen Wang

Beijing Key Laboratory of Green Reaction Engineering and Technology, Department of Chemical Engineering, Tsinghua University, Beijing 100084, China

ARTICLE INFO

Article history:
Received 26 September 2009
Received in revised form 28 March 2010
Accepted 29 March 2010

Keywords:
Airlift reactor
Mass transfer
Bubble size distribution
Interfacial area
Non-Newtonian fluid

ABSTRACT

Gas holdup, bubble behavior, interfacial area and gas–liquid mass transfer in a 5 m internal-loop airlift reactor with non-Newtonian fluid were studied in the superficial gas velocity (U_g) range of 2–12 cm/s. Air and aqueous CMC solutions of 0–0.45 wt% were used as the gas and liquid phases, respectively. It was found that increased U_g or CMC concentration led to a wider bubble size distribution and an increase in the bubble Sauter diameter. The volumetric mass transfer coefficient increased with an increase in U_g and a decrease in CMC concentration. In the air–water system, k_la/α_g was found to be independent of U_g and was 0.2 1/s, and a constant liquid-side mass transfer coefficient (k_l) was found in the heterogeneous regime. However, in the air–CMC solution system, the influences of the superficial gas velocity and liquid viscosity were much more complicated: k_la/α_g was not constant and was affected by the superficial gas velocity and CMC concentrations; the interfacial area increased with an increase in U_g and a decrease in CMC concentration; k_l increased more significantly with increasing U_g, and no obvious trend was found for the influence of CMC concentration on k_l.

1. Introduction

Airlift reactors are widely used in chemical and biochemical industrial processes, because of their simple construction, good heat transfer, low shear rate, low power input and easy scale up [1,2]. Mass transfer is one of the most significant factors in process design and reactor scale up, and has been intensively studied in airlift reactors during the past decades [3–9]. However, most of these studies have focused on experimental determination of the volumetric mass transfer coefficient (k_la), which is a global parameter that depends on reactor geometry, operating conditions and phase properties [7,10–14]. The common approach to describe k_la is to correlate it with the factors that affect it. The separation of liquid-side mass transfer coefficient (k_l) and interfacial area (a) can allow the identification of whether k_l or a controlled the mass transfer rate. However, only a few investigations focus on such improvement [9,15–18]. In this work, we performed this study on the influence of non-Newtonian fluid.

In fact, the mass transfer rate in an airlift reactor depends on gas holdup, flow regime, bubble size distribution, bubble breakup and coalescence, interfacial area and liquid-side mass transfer coefficient [19]. Further, local measurements of these parameters are needed because they can provide much more details than global measurements [1,20,21], and can be used for validations of computational fluid dynamics (CFD) simulations [22].

The reactor size has a significant influence on the hydrodynamics and mass transfer rate [14,23–25]. It is commonly accepted that the hydrodynamics becomes independent of the column size only when the column diameter (D), column height (H), and aspect ratio (H/D) are larger than certain threshold values [2]. Wilkinson et al. [26] suggested that H should be larger than 1–3 m. However, most works on the airlift reactor in the literature have used reactors of about 2 m [10,13,27,28], and only some works have used a reactor of 4 m high [5,6,29,30]. Therefore, an investigation using a larger airlift reactor will be valuable for a better understanding of the scale up behavior. In addition, most works on airlift reactor in the literature has been carried out with Newtonian fluid and much limited attention has been paid on studies of non-Newtonian or high viscosity liquid systems [15,27,31–34], despite the fact that in many chemical reactors the fluids have a relatively high viscosity or exhibit non-Newtonian behavior [35]. Different from that of Newtonian fluid, the viscosity of non-Newtonian fluid is dependent of shear rate. For instance, the viscosity of the shear thinning non-Newtonian fluids decreases when shear rate increases [36]. Further, the results in the literature are still not enough for a better understanding on the influence of non-Newtonian fluid. For example, Li et al. [32] studied the influence of non-Newtonian fluid on the hydrodynamics and mass transfer using a wide range CMC concentration of 1–4% in a 3.9 m high internal airlift reactor. However, this work was limited to experimental determination of k_la

* Corresponding author. Tel.: +86 10 62797490, fax: +86 10 62772051.
E-mail addresses: wangtf@tsinghua.edu.cn, wangtf@flotu.org (T. Wang).

1385-8947/$ – see front matter © 2010 Elsevier B.V. All rights reserved.
doi:10.1016/j.cej.2010.03.078

Nomenclature

Notations

a_l	gas–liquid interfacial area per unit liquid volume, m^{-1}
a_{large}	gas–liquid interfacial area of large bubble, m^{-1}
a_{small}	gas–liquid interfacial area of small bubble, m^{-1}
a	gas–liquid interfacial area per unit dispersion volume, m^{-1}
A_d	cross-sectional area of the downcomer, m^2
A_r	cross-sectional area of the annular riser, m^2
C_l	oxygen concentration in the liquid, kg/m^3
C_l^*	saturation oxygen concentration in the liquid, kg/m^3
C_{sensor}	liquid phase oxygen concentration given by sensor, kg/m^3
d_b	bubble diameter, m
d_S	bubble Sauter diameter, m
h	height, m
K	consistency index, Pa s^n
k_l	liquid-side mass transfer coefficient, m/s
k_{large}	liquid-side mass transfer coefficient of large bubble, m/s
k_{small}	liquid-side mass transfer coefficient of small bubble, m/s
k_{sensor}	sensor time constant, s^{-1}
k_la	volumetric mass transfer coefficient based on dispersion volume, s^{-1}
k_la_l	volumetric mass transfer coefficient based on liquid volume, s^{-1}
n	flow index, arbitrary units
P	pressure, Pa
t	time, s
U_g	superficial gas velocity, cm/s
U_{gr}	superficial gas velocity in the riser, cm/s

Greek symbols

α_g	gas holdup, arbitrary units
α_{gd}	gas holdup in the downcomer, arbitrary units
α_{gr}	gas holdup in the riser, arbitrary units
γ	shear rate, s^{-1}
μ_{app}	apparent viscosity, Pa s
τ	shear force, N/m^2
ρ_l	liquid density, kg/m^3

Subscripts

d	downcomer
g	gas phase
l	liquid phase
r	riser

and the reactor used a single-hole sparger, which was not usually adopted in industrial reactors. Therefore, the investigation on the influence of non-Newtonian fluid is needed, especially in a large airlift reactor.

This work studied the gas holdup, bubble behavior and gas–liquid mass transfer rate in a 5 m high internal-loop airlift reactor with water and aqueous solution of carboxyl methyl cellulose (CMC). The influences of the CMC concentration and superficial gas velocity (U_g) on the global and local gas holdup, bubble size distribution, volumetric mass transfer coefficient, interfacial area and liquid-side mass transfer coefficient were investigated.

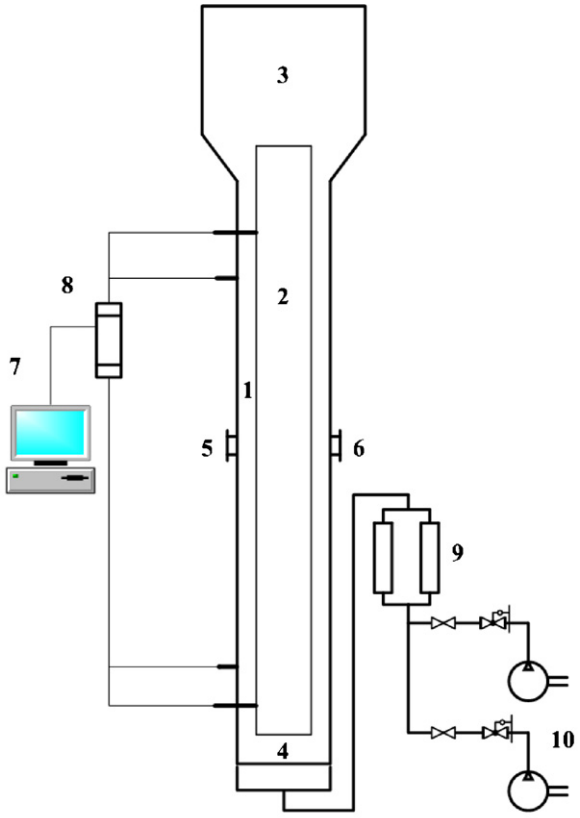

1. Riser; 2. Downcomer; 3. Separator; 4. Gas distributor;

5. Electrical conductivity probe port; 6. Oxygen probe port; 7. PC;

8. Differential pressure transducer; 9. Flow meter; 10. Compressor.

Fig. 1. Schematic of the experimental set-up.

2. Experimental

2.1. Experimental apparatus

The schematic of the experimental apparatus is shown in Fig. 1. The internal-loop airlift reactor used was made of Plexiglas. It comprised four main parts: annular riser, downcomer, gas–liquid separator and gas distributor. The total height of the reactor was 5 m. The riser was 0.28 m inner diameter (i.d.), and 4.1 m high. The separator was 0.48 m i.d., and 0.9 m high. The draft tube was 0.19 m outer diameter, 0.18 m i.d., and 4.0 m high. The gas distributor was an annular perforated plate with 196 holes of 1 mm diameter, thus the gas was only injected into the annular riser.

2.2. Physical properties

Air was used as the gas phase. Tap water and aqueous CMC solution of 0.2–0.45 wt% were used as the liquid phase. The apparent viscosity of the CMC solutions was measured by a viscometer, and can be expressed as [37]:

$$\mu_{app} = \frac{\tau}{\gamma} = K\gamma^{n-1} \quad (1)$$

where K is the consistency index, and n is the flow index. The measured values of K and n are listed in Table 1. To illustrate the characteristic viscosity of the liquid phase, the apparent viscosities at the shear rate of 200 s^{-1} are also listed in Table 1.

Table 1
Phase properties of CMC solution.

Concentration, wt%	Density, kg/m^3	K, Pa s^n	n	μ (γ = 200 s^{-1}), Pa s
0.2	1001.5	0.0065	0.955	0.0051
0.3	1002.5	0.0209	0.911	0.0130
0.4	1003.5	0.0487	0.823	0.0191
0.45	1004.0	0.0973	0.732	0.0235

2.3. Measuring method

2.3.1. Global gas holdup

The global gas holdups in the riser and downcomer were measured with the pressure drop method. Both the riser and downcomer had two tap ports at 0.4 m and 3.6 m above the gas distributor. Differential pressure transducers were used to measure the pressure drop. The sampling frequency was 10 Hz. In most gas–liquid flows, the pressure drop due to the viscosity can be neglected compared to static pressure drop, and the pressure drop (ΔP) between the two tap ports with vertical distance of h is [38]:

$$\Delta P = \rho_l g h(1-\alpha_g) \tag{2}$$

where ρ_l is the liquid density and α_g is the gas holdup.

The pressure drops in the riser (ΔP_r) and downcomer (ΔP_d) were measured through the taping ports connected to them. From the measured ΔP_r and ΔP_d, the gas holdups in the riser (α_{gr}) and downcomer (α_{gd}) could be respectively determined from Eq. (2).

The global gas holdup in the reactor is:

$$\alpha_g = \frac{\alpha_{gr}A_r + \alpha_{gd}A_d}{A_r + A_d} \tag{3}$$

where A_r and A_d are the cross-sectional area of the annular riser and downcomer, respectively.

2.3.2. Bubble behavior and local gas holdup

The bubble characteristics and local gas holdup were measured 2.0 m above the gas distributor with a dual-tip electrical conductivity probe, which is shown in Fig. 1. The distance between the two tips was 1.25 mm. The measuring principle was based on the different conductivities of the gas and liquid, which gave different output voltage signals when the probe tip was in contact with different phases. The bubble chord length, rise velocity, size distribution and local gas holdup were obtained from the measured signals by the use of a previously published algorithm [39].

2.3.3. Mass transfer

The volumetric mass transfer coefficient k_la was determined by the oxygen desorption technique. An oxygen probe (LDO^{TM} HQ10, HACH Company, U.S.A.) placed at 2.0 m above the gas distributor was used to measure the change in oxygen concentration with time. The sensor constant was calibrated by switching the sensor environment from a nitrogen-saturated liquid to an air-saturated liquid [40]. Assuming that the probe has a first order response and the liquid phase was perfectly mixed, the oxygen concentration measured by the sensor in an air-saturated liquid, C_{sensor}, can be calculated using:

$$\frac{dC_{sensor}}{dt} = k_{sensor}(C_l^* - C_{sensor}) \tag{4}$$

where k_{sensor} was time constant of the sensor, and C_l^* is the oxygen value when the probe had been put in the air-saturated liquid for a long enough time. The results showed that k_{sensor} changed only slightly in the ranges of the gas velocity and liquid viscosity used in this work. Thus, an average value of k_{sensor}, which was 0.1 s^{-1}, was used for convenience. The CSTR model was used to determine k_la. Assuming that the liquid was perfectly mixed and oxygen accumulation in the gas phase was negligible, the mass transfer rate measured by the sensor was given by [41]:

$$\frac{C_{sensor}}{C_l^*} = \frac{1}{k_{sensor} - k_1a_1}[k_{sensor}e^{-k_1a_1t} - k_1a_1e^{-k_{sensor}t}] \tag{5}$$

where k_la_l was the volumetric mass transfer coefficient per unit volume of liquid. The relationship between k_la_l and k_la was:

$$k_1a_1 = \frac{k_1a}{(1-\alpha_g)} \tag{6}$$

It should be pointed out that there was a difference between the mass transfer rates in the riser and in the downcomer. The volumetric mass transfer coefficient measured in this work was a global value of the whole reactor. Then k_la was determined by fitting the experimental curve to Eqs. (5) and (6). The liquid-side mass transfer coefficient was determined by:

$$k_1 = \frac{k_1a}{a} \tag{7}$$

where a was the interfacial area, which was calculated using:

$$a = \frac{6\alpha_g}{d_S} \tag{8}$$

3. Results and discussion

3.1. Gas holdup

3.1.1. Global gas holdup

Fig. 2(a)–(c) shows the influence of U_g and CMC addition on the gas holdups in the riser, downcomer and the overall reactor. The value of U_g for flow regime transition was about 5 cm/s in the air–water system, and decreased to about 4 cm/s in highly viscous media. In the homogenous regime, the gas holdup increased linearly with U_g; while in the heterogeneous regime, the increase of gas holdup slowed down due to bubble coalescence. These results were in agreement with the study of Hwang and Cheng [42]. Fig. 2 also indicates that the gas holdup decreased with an increase in CMC concentration. There were more large bubbles in the viscous liquid. Large bubbles had a short residence time, thus led to a decrease in the gas holdup [34]. It should be noted that the gas holdups in 0.4 wt% and 0.45 wt% CMC solutions were quite similar at $U_g \leq 6$ cm/s. Similar phenomena were also found in the literature. The study of Hwang and Cheng [42] showed that the gas holdup in the downcomer in 0.8 wt% CMC solution was higher than that in 0.5 wt% CMC solution. The study of Fransolet et al. [36] showed that the gas holdups were close in the 4 wt% and 5 wt% xanthan solutions at $U_g \leq 8$ cm/s. The reason was two opposing folds: one was that the bubble rise velocity decreased with an increase in liquid viscosity, which led to a longer bubble residence time and a higher gas holdup; the other was that the bubble rise velocity increased with an increase in bubble diameter, which in turn increased with an increase in liquid viscosity due to reduced bubble breakup. At $U_g \leq 6$ cm/s, with an increase in liquid viscosity, the decrease in gas holdup due to increased bubble diameter was counteracted by the effect of decreased bubble velocity. Thus, the gas holdups in 0.45 wt% were similar to that in 0.4 wt% CMC solution. While at $U_g > 6$ cm/s, bubble coalescence and breakup became more intensive, and the increase in bubble diameter caused by increased liquid

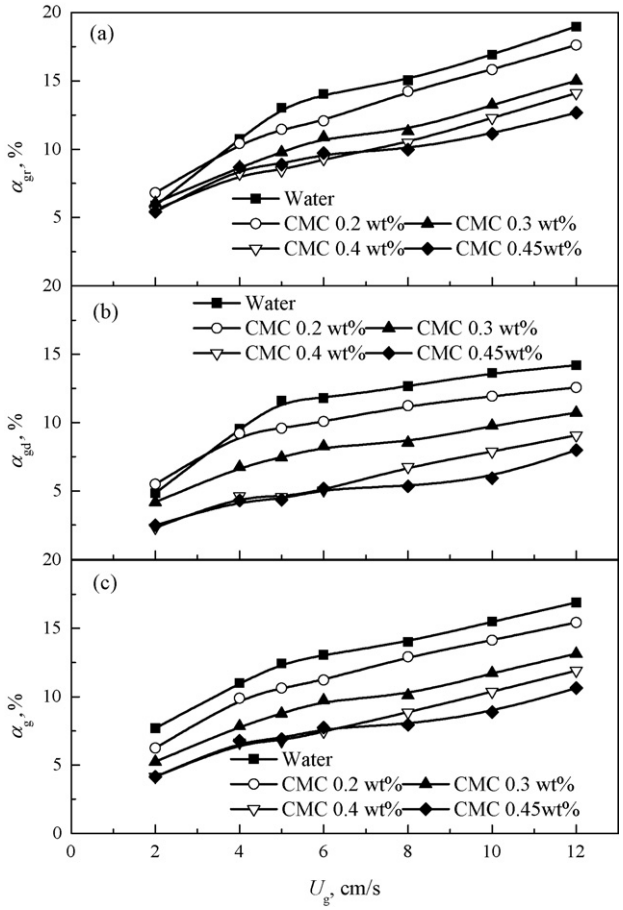

Fig. 2. Effects of superficial gas velocity and CMC concentration on gas holdup (a) riser; (b) downcomer; (c) overall.

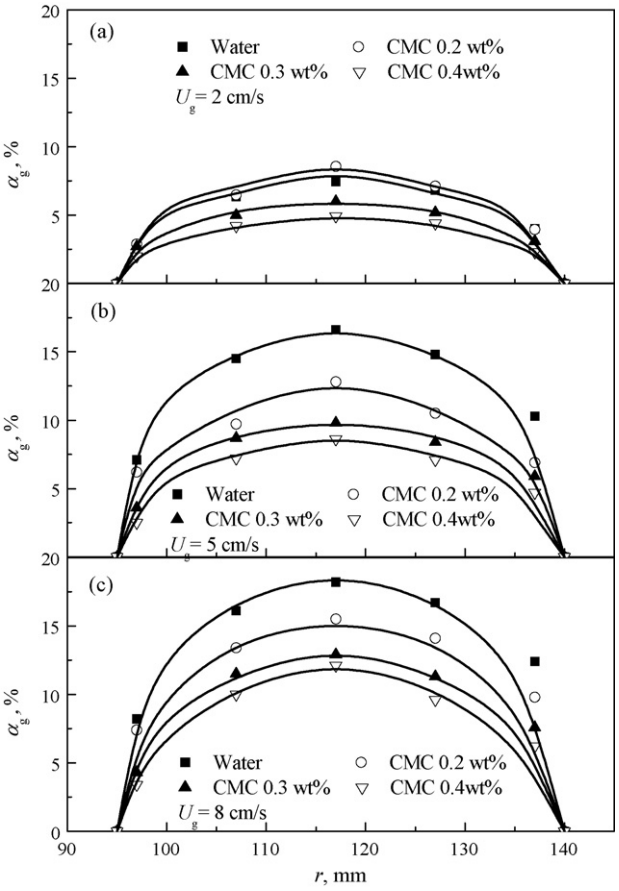

Fig. 4. Effect of CMC concentration on radial profile of gas holdup in riser.

viscosity was dominant. As a result, the gas holdup in 0.45 wt% CMC solution was lower than that in 0.4 wt% solution. The gas holdups in the riser and downcomer for water, 0.3 wt% and 0.45 wt% CMC solutions are shown in Fig. 3. It was found that the difference between gas holdups in the riser and downcomer increased with an increase in CMC concentration. The increased CMC concentration (apparent viscosity) led to an increase in the fraction of large bubbles that passed through the riser without being entrained into the downcomer. Thus, the gas holdup in the downcomer decreased and the difference between gas holdups in the riser and downcomer increased.

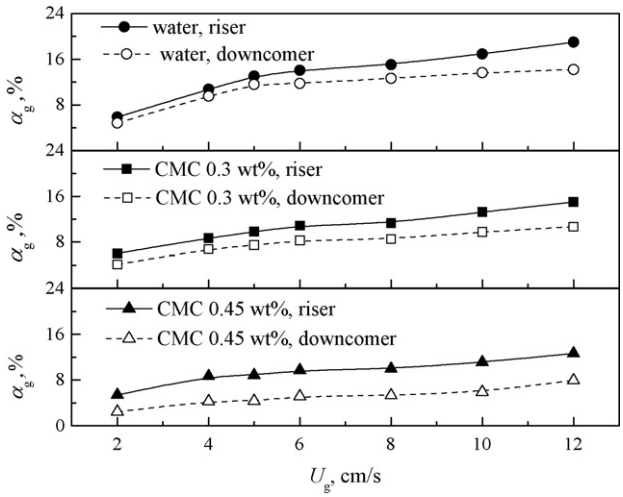

Fig. 3. Effect of CMC concentration on difference between gas holdups in riser and downcomer.

3.1.2. Local gas holdup

The influences of U_g and CMC concentration on the radial profiles of the gas holdup in the riser are shown in Fig. 4(a)–(c). The radial profiles of the gas holdup were quite flat at a low U_g and became much non-uniform at a high U_g. The radial profile of the gas holdup was determined by the lateral forces on gas bubbles exerted by the liquid flow. The lateral forces include the later lift force, turbulent dispersion force, and wall lubrication force. It has been reported that in a bubble column, bubbles larger than 5.8 mm are exerted a negative lift force and migrate toward the reactor center, while bubbles smaller than 5.8 mm are exterted a positive lift force and migrate toward the reactor wall [43,44]. The turbulent dispersion force is due to the gas holdup profile and flow turbulence, and tends to smooth the radial profile of the gas holdup. At U_g = 2 cm/s, the reactor was in the homogenous regime and the bubble coalescence was negligible, thus the bubble size distribution was relatively narrow, with a smaller Sauter diameter. In this regime, the radial profile of the gas holdup was significantly affected by the gas distributor. While at U_g = 8 cm/s, the reactor was in the heterogeneous regime and bubble coalescence was frequent, thus the bubble size distribution was wider and the Sauter diameter was larger. The lift force acted on large bubbles forced them to migrate toward the reactor center and when the lift force and the turbulent dispersion force reached a balance, a parabolic profile was formed. This analysis was also confirmed by the discussion on the bubble size distribution in Section 3.2.1.

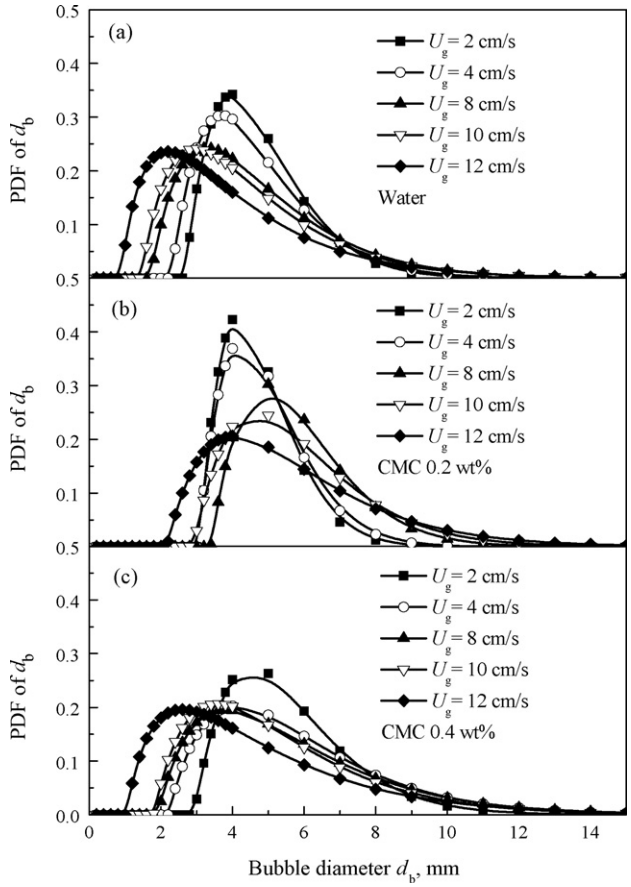

Fig. 5. Effect of superficial gas velocity on bubble size distribution.

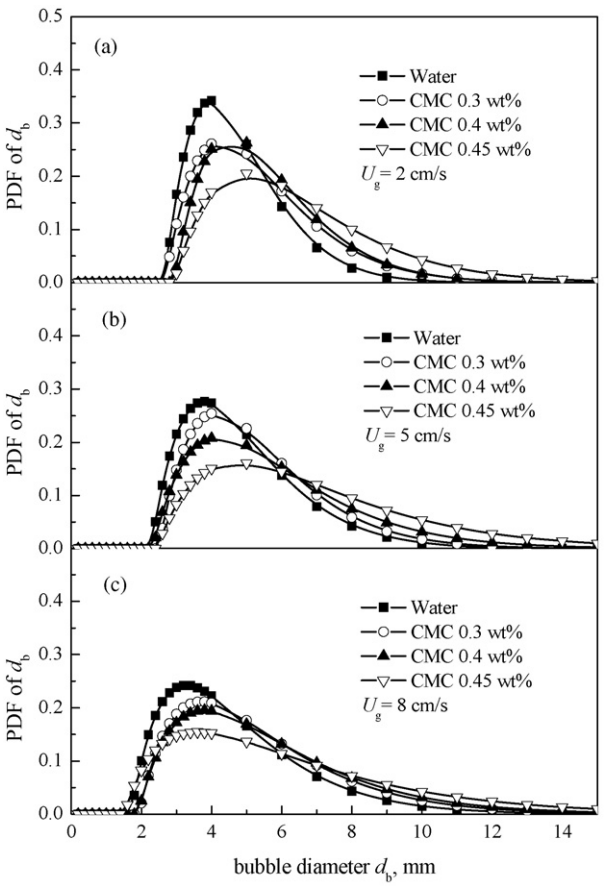

Fig. 6. Effect of CMC concentration on bubble size distribution.

3.2. Bubble behavior

3.2.1. Bubble size

The bubble behavior was measured 2 m above the gas distributor, where the flow was fully developed. Bubble size distribution is determined by the gas distributor, phase physical properties, operating conditions, and reactor geometry [45,46]. Fig. 5(a)–(c) show the influence of U_g on the bubble size distribution for water, and 0.2 wt% and 0.4 wt% CMC solutions, respectively. The distribution was relatively narrow at a low U_g, and became wider with an increase in U_g. These are in agreement with the results in the literature [47,48]. In the homogenous regime, gas holdup and turbulence intensity were low, thus bubble breakup and coalescence were negligible, and the bubble size distribution was mainly determined by the gas distributor and liquid properties. In the heterogeneous regime, bubble breakup and coalescence were quite frequent. As a result, a wider bubble distribution was obtained where bubble breakup was balanced by bubble coalescence.

The influence of CMC concentration on the bubble size distribution for three U_g is shown in Fig. 6. The bubble size distribution increased with an increase in CMC concentration. For instance, at U_g = 2 cm/s, the bubble size ranged from 2.8 mm to 13 mm in the air/water system; while bubbles larger than 18 mm appeared in the 0.45 wt% CMC solution. The increase in CMC concentration (liquid viscosity) led to a decrease in turbulence intensity, which in turn decreased the bubble breakup and coalescence. Further, the bubble breakup was more sensitive to liquid viscosity than bubble coalescence, thus the bubble size distribution shifted to larger size with an increase in CMC concentration. The researches on the bubble coalescence show that there are three main mechanisms, namely bubble coalescence due to turbulent eddies, different bubble rise velocities and bubble wake entrainment [22]. The spherical cap bubbles formed at U_g = 2 cm/s were mainly due to the coalescence due to different rise velocities. In addition, with the low turbulence intensity due to low U_g and high liquid viscosity, bubble breakup is very weak and these spherical cap bubbles could stably exist, though with a few number.

The influence of U_g on the bubble Sauter diameters is shown in Fig. 7. The bubble Sauter diameter slightly increased with an increase in U_g, and significantly increased with an increase in CMC concentration. Yoshimoto et al. [15] also found that bubble Sauter

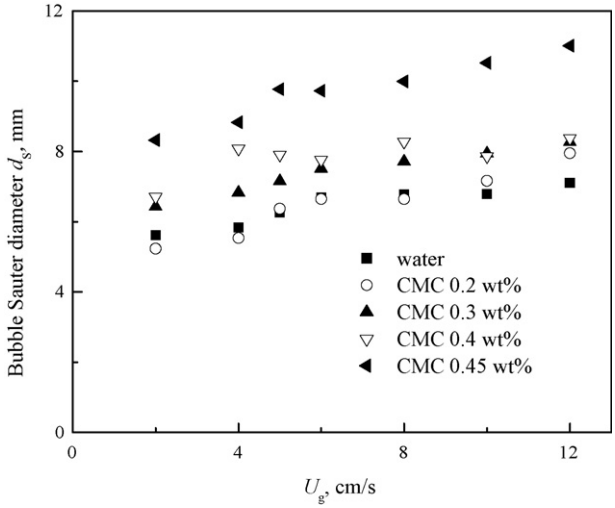

Fig. 7. Effects of superficial gas velocity and CMC concentration on Sauter diameter.

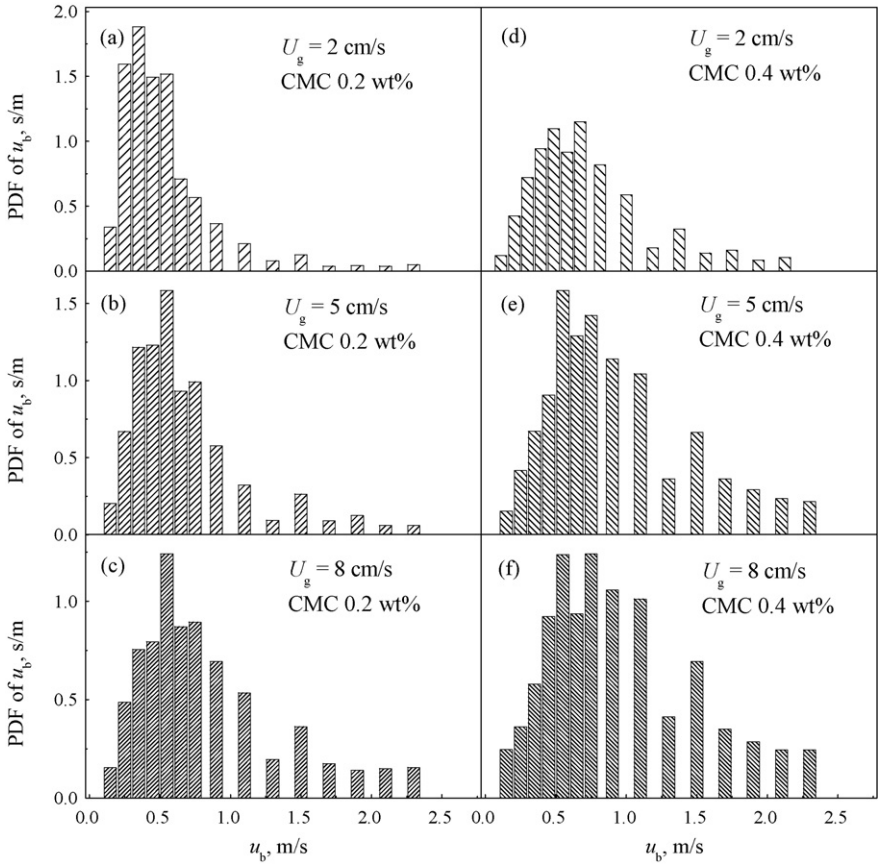

Fig. 8. Effects of superficial gas velocity and CMC concentration on bubble velocity distribution.

diameter increased with an increase in liquid viscosity but was approximately independent of U_g.

3.2.2. Bubble rise velocity

The bubble rise velocity affects the gas holdup and the residence time of gas phase. With an increase in U_g, the bubble rise velocity increased and its distribution became wider and bimodal distributions emerged in a high U_g, or even emerged in a low U_g in a highly viscous CMC solution, as shown in Fig. 8. The influence of U_g on the bubble rise velocity in an airlift reactor was associated with bubble wake effect. When the gas holdup increased with U_g, the bubble number within a bubble swarm also increased, which resulted in a decrease in the drag force and an increase in the bubble rise velocity. On the other hand, an increased U_g enhanced flow turbulence and bubble breakup and coalescence, and resulted in a wider distribution of the bubble rise velocity. The two peaks of the bimodal distributions mainly appeared at 0.5–0.75 m/s and 1.5 m/s, which are corresponding to the small bubble (<10 mm) velocity and spherical cap bubble velocity, respectively. It is noted that the rise velocity of spherical cap bubbles was unchanged, in agree with the research of Krishna and Ellenberger [49] that showed the rise velocity of large bubble were not influence by liquid properties. The bimodal distribution of bubble rise velocity appeared at a low U_g in a highly viscous CMC solution, as shown in Fig. 8(d). This was agreed with the data of bubble size distribution, which showed that spherical cap bubbles emerged even at a low U_g in a higher CMC concentration. In general, the bubble rise velocity was influenced by the local gas holdup, bubble size and liquid velocity. A higher CMC concentration led to bimodal distributions of the bubble size and bubble rise velocity. Fig. 9 shows the influence of U_g and CMC concentration on the average bubble rise velocity. The average bubble rise velocity increased with an increase in U_g and a decrease in CMC concentration. It is noted that the bubble velocities in 0.45 wt% CMC solution in the heterogeneous regime was almost unchanged. This phenomenon can be interpreted as follows. The bubble rise velocity measured in this work was the absolute velocity, which was the sum of the liquid velocity and bubble slip velocity. The bubble velocity was more sensitive to liquid velocity because the variations of slip velocity for 2–10 mm bubbles were relative small. An estimation of the variation of liquid velocity could be made from

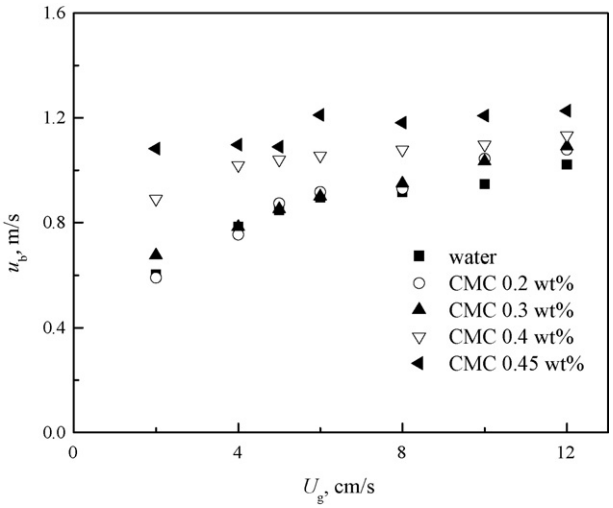

Fig. 9. Effects of superficial gas velocity and CMC concentration on average bubble rise velocity.

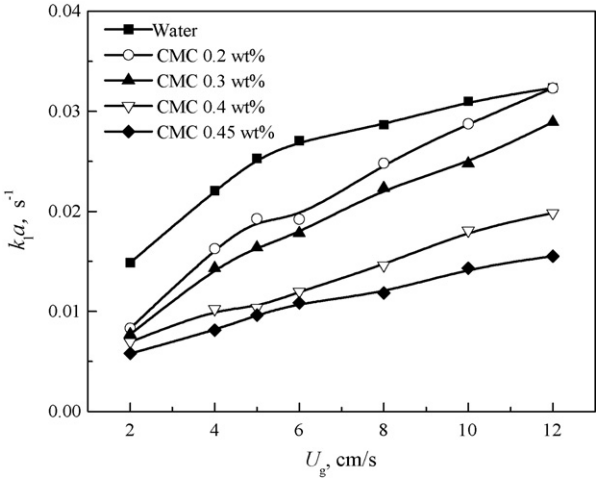

Fig. 10. Effects of superficial gas velocity and CMC concentration on $k_l a$.

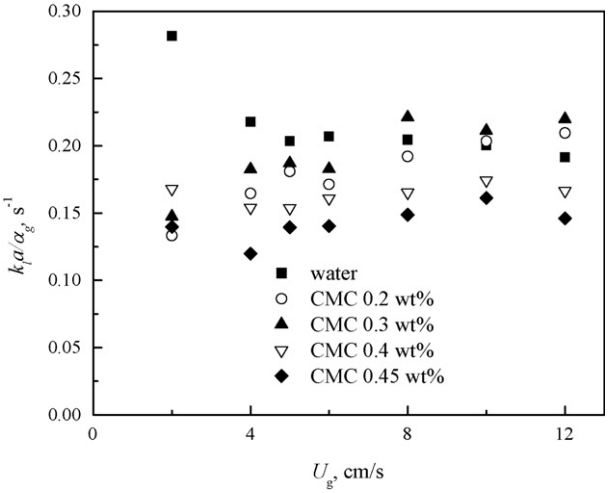

Fig. 11. Variation of $k_l a/\alpha_g$ with U_g and CMC concentration.

the difference of gas holdup in the riser and downcomer. Fig. 3 showed that the difference of gas holdup increased with increased U_g in low CMC solutions, which indicated that the liquid velocity increased with an increase in U_g. While in a high CMC solution, the difference of gas holdup remained constant in the heterogeneous regime, which indicated that the liquid velocity remained constant in the heterogeneous regime. Since the bubble velocity was more sensitive to the liquid velocity, the bubble velocity was almost unchanged in the heterogeneous regime in 0.45 wt% CMC solution.

3.3. Mass transfer rate

3.3.1. Volumetric mass transfer coefficient

The effects of U_g and CMC concentration on $k_l a$ are shown in Fig. 10. The results show that $k_l a$ increased with an increase in U_g and a decrease in CMC concentration. In water or a CMC solution of low concentration, $k_l a$ showed different variations with U_g in different ranges, with a critical U_g of 5 cm/s. Above this critical U_g, the increase of $k_l a$ became less significant, which was considered as the different mass transfer behaviors in the homogenous and heterogeneous regimes. While in a CMC solution of high concentration, no clear transition was found for $k_l a$. This was in agreement with the results in the literature that the heterogeneous regime prevails at a highly viscous liquid even at a low superficial gas velocity [50].

The gas–liquid mass transfer rate is closely related to the hydrodynamics, e.g., the variation of $k_l a$ is similar to that of the gas holdup. Letzel and Stankiewicz [51] reported that the ratio $k_l a/\alpha_g$ in the nitrogen–water system was almost constant and was 0.5 1/s at different system pressures. Jordan and Schumpe [52] also reported that $k_l a/\alpha_g$ in the nitrogen–decalin system was almost independent of U_g and gas density, and was 0.45 1/s. Vandu and Krishna [25] reported that $k_l a/\alpha_g$ in the air–water system was 0.48 1/s, and was practically independent of the column diameter and U_g. These results are interesting and significant, for they indicate a simple rule that can be used to estimate $k_l a$ from the gas holdup. The measurement of the gas holdup is much easier than that of $k_l a$. However, this simple correlation still needs more validation with various liquid properties and with different reactor types. The variation of $k_l a/\alpha_g$ with U_g in this work is shown in Fig. 11. In the air–water system, the value of $k_l a/\alpha_g$ was almost independent of U_g and was 0.2 1/s. This value was lower than that reported in the literature, which was probably due to the different type and geometry of reactor used. The reactor used in this work was a 5 m high internal airlift reactor. The small bubbles recirculated in the reactor, and contributed significantly to gas holdup but insignificantly to mass transfer. This was because the limited oxygen in these small bubbles can be rapidly depleted in the riser and only small bubbles can enter the downcomer. The volumetric mass transfer coefficient determined by the CSTR model was based on the volume of the whole reactor, therefore $k_l a$ and the value of $k_l a/\alpha_g$ in this work were much smaller than that in the bubble column reported in the literature. With the addition of CMC, the conditions became more complicated. In the 0.4 wt% CMC solution, $k_l a/\alpha_g$ was about 0.16; and in the 0.45 wt% CMC solution, this value was about 0.14. However, $k_l a/\alpha_g$ was not constant in the 0.2 wt% and 0.3 wt% CMC solutions, but slightly increased with an increase in U_g.

3.3.2. Interfacial area and liquid-side mass transfer coefficient

The interfacial area a calculated by Eq. (8) is shown in Fig. 12. In general, a showed a similar variation to that of $k_l a$, i.e., increased with an increase in U_g and a decrease in CMC concentration. The increase of a with U_g was more significant in the homogenous regime than in the heterogeneous regime, especially at a low liquid viscosity. Stegeman et al. [53] reported similar results in a bubble column, and concluded that the flow regime had an important influence on the mode in which the operating parameters affected the interfacial area.

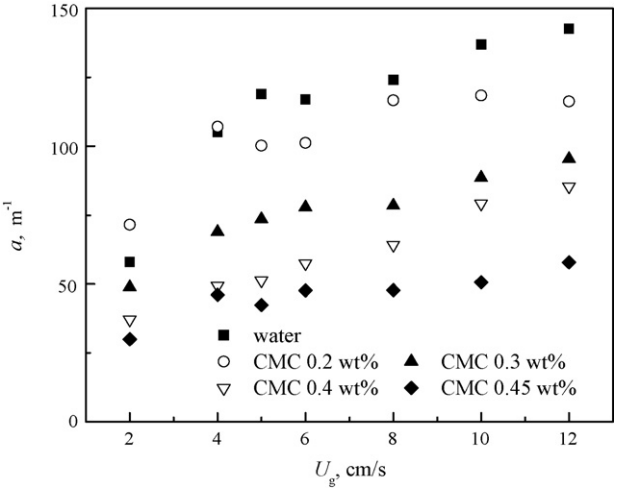

Fig. 12. Effects of superficial gas velocity and CMC concentration on gas–liquid interfacial area.

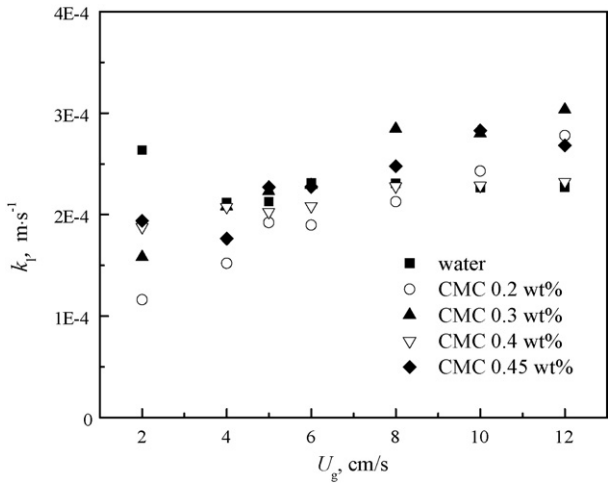

Fig. 13. Effects of superficial gas velocity and CMC concentration on liquid-side mass transfer coefficient.

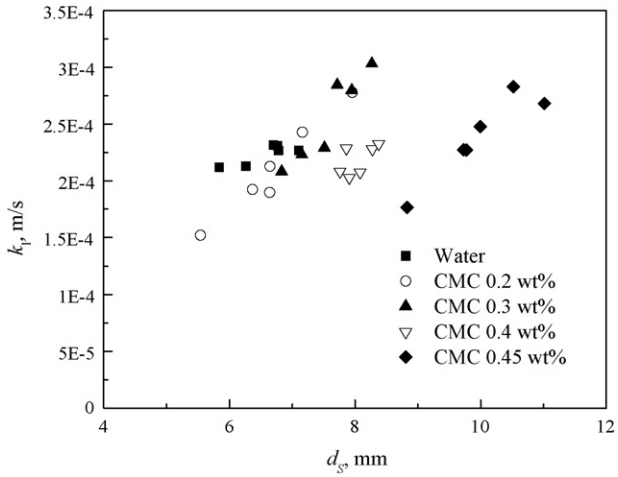

Fig. 14. Effect of bubble Sauter diameter on k_l.

The variation of k_l with U_g and CMC concentration is shown in Fig. 13. In the air–water system, k_l was only slightly affected by U_g and was 2.2×10^{-4} m/s in the heterogeneous regime. With the addition of CMC, k_l increased more significantly with increasing U_g, except in the solution of 0.4 wt% CMC. For example, k_l in the solution of 0.2 wt% CMC increased from 1.2×10^{-4} to 2.8×10^{-4} m/s when U_g increased from 2.0 cm/s to 12.0 cm/s. The effect of CMC solution on k_l is rather complex and no simple rule could be made. Note that some data were intercrossed under the similar conditions. This was caused by measurement error. Due to the limitation of indirect measurement, the measurement uncertainties of interfacial area and liquid-side mass transfer coefficient were up to 20%. Considering the measurement uncertainty, the estimation errors of the liquid-side mass transfer coefficient are sometimes larger than the variations with U_g.

Different results on the influence of liquid viscosity and U_g on k_l have been reported in the literature. The study of Yoshimoto et al. [15] showed that k_l decreased with an increase in liquid viscosity, while the study of Maalej et al. [54] showed that k_l decreased for low U_g and remain constant for high U_g. Yang et al. [55] reported that both the interfacial area and mass transfer coefficient increased with increasing superficial gas and liquid velocities. The complex variation of k_l was discussed as below. Vandu et al. [56] reported that k_l for large bubbles was practically independent of the superficial gas velocity and had a value in the range of 0.002–0.003 m/s, about 1 order of magnitude higher than the average k_l in this work. This higher k_l value can be attributed to the frequent bubble breakup and coalescence of large bubbles that enhance the renewal of the gas–liquid interface. Thus with the addition of CMC, the average k_l may be estimated by:

$$k_1 = \frac{k_{large}a_{large} + k_{small}a_{small}}{a_{large} + a_{small}} \quad (9)$$

where the subscripts "large" and "small" are for the large and small bubbles. Eq. (9) indicates that k_l depends on the bubble Sauter diameter. Here it is assumed that the concentrations are the same in large and small bubbles. Fig. 14 showed the effect of the bubble Sauter diameter on k_l. It can be seen that k_l increased with an increase in the bubble Sauter diameter for each solution, and decreased with an increase in CMC concentration. The reason is that bubble breakup and coalescence are more intensive for large bubbles and low CMC concentrations. Thus, the complex influence of CMC concentration on k_l was a joint behavior of two opposing folds. First, the flow turbulence decreased with an increase in CMC concentration and led to a lower k_l. Second, the number of large bubbles which had a larger k_l increased with an increase CMC concentration. However, for strict and quantitative discussion, further study with more advanced measurement is needed.

4. Conclusions

The gas holdup, bubble behavior, interfacial area and gas–liquid mass transfer in a 5 m high internal-loop airlift reactor with non-Newtonian fluid were studied. The effects of the superficial gas velocity and CMC concentration on the global and local gas holdups, bubble size distribution, bubble velocity, volumetric mass transfer coefficient, interfacial area and liquid-side mass transfer coefficient were obtained. The main conclusions were:

(1) Global gas holdup increased with an increase in superficial gas velocity (U_g) and a decrease in CMC concentration. The radial profile of the gas holdup in riser became more non-uniform with an increase in the average gas holdup.
(2) The bubble size distribution became wider with a larger Sauter diameter with an increase in U_g and CMC concentration. The bubble rise velocity increased with an increase in U_g and CMC concentration.
(3) The volumetric mass transfer coefficient increased with an increase in U_g and a decrease in CMC concentration. The value of $k_l a/\alpha_g$ was 0.2 1/s in the air–water system, and it depended on U_g and CMC concentration in CMC solutions.
(4) The interfacial area increased with an increase in U_g and a decrease in CMC concentration, and the flow regime had a significant effect on the interfacial area. In the air–water system, the liquid-side mass transfer coefficient (k_l) was almost independent of U_g and was 2.2×10^{-4} m/s in the heterogeneous regime. In the CMC solutions, k_l increased more significantly with increasing U_g. No obvious trend was found for the influence of CMC concentration on k_l.

Acknowledgements

The authors gratefully acknowledge the financial supports by Foundation for the Author of National Excellent Doctoral Dissertation of PR China (no. 200757), and National 973 Project of China (no. 2007CB714302).

References

[1] H.P. Luo, M.H. Al-Dahhan, Local characteristics of hydrodynamics in draft tube airlift bioreactor, Chemical Engineering Science 63 (2008) 3057–3068.
[2] T.F. Wang, J.F. Wang, Y. Jin, Slurry reactors for gas-to-liquid processes: a review, Industrial & Engineering Chemistry Research 46 (2007) 5824–5847.
[3] S.J. Hwang, W.J. Lu, Gas–liquid mass transfer in an internal loop airlift reactor with low density particles, Chemical Engineering Science 52 (1997) 853–857.
[4] M. Blazej, M. Jurascik, J. Annus, J. Markos, Measurement of mass transfer coefficient in an airlift reactor with internal loop using coalescent and non-coalescent liquid media, Journal of Chemical Technology and Biotechnology 79 (2004) 1405–1411.
[5] K. Nakao, S. Suenaga, K. Furumoto, M. Yoshimoto, K. Fukunaga, Hydrodynamic and mass transfer properties in a three phase external loop airlift compared with a three phase internal loop airlift and a slurry bubble column, Chemical and Biochemical Engineering Quarterly 21 (2007) 373–381.
[6] J.P. Giovannettone, J.S. Gulliver, Gas transfer and liquid dispersion inside a deep airlift reactor, AIChE Journal 54 (2008) 850–861.
[7] G.Q. Li, S.Z. Yang, Z.L. Cai, J.Y. Chen, Mass-transfer and gas–liquid circulation in an airlift bioreactor with viscous non-Newtonian fluids, Chemical Engineering Journal and the Biochemical Engineering Journal 56 (1995) B101–B107.
[8] X.P. Lu, J. Ding, Y.R. Wang, J. Shi, Comparison of the hydrodynamics and mass transfer characteristics of a modified square airlift reactor with common airlift reactors, Chemical Engineering Science 55 (2000) 2257–2263.
[9] G. Dursun, C. Akosman, Gas–liquid interfacial area and mass transfer coefficient in a co-current down flow contacting column, Journal of Chemical Technology and Biotechnology 81 (2006) 1859–1865.
[10] P.M. Kilonzo, A. Margaritis, M.A. Bergougnou, J.T. Yu, Q. Ye, Effects of geometrical design on hydrodynamic and mass transfer characteristics of a rectangular-column airlift bioreactor, Biochemical Engineering Journal 34 (2007) 279–288.
[11] N. El Azher, B. Gourich, C. Vial, M.S. Bellhaj, A. Bouzidi, M. Barkaoui, M. Ziyad, Influence of alcohol addition on gas hold-up, liquid circulation velocity and mass transfer coefficient in a split-rectangular airlift bioreactor, Biochemical Engineering Journal 23 (2005) 161–167.
[12] A. Fadavi, Y. Chisti, Gas–liquid mass transfer in a novel forced circulation loop reactor, Chemical Engineering Journal 112 (2005) 73–80.
[13] S. Krichnavaruk, P. Pavasant, Analysis of gas–liquid mass transfer in an airlift contactor with perforated plates, Chemical Engineering Journal 89 (2002) 203–211.
[14] F. Benyahia, L. Jones, Scale effects on hydrodynamic and mass transfer characteristics of external loop airlift reactors, Journal of Chemical Technology and Biotechnology 69 (1997) 301–308.
[15] M. Yoshimoto, S. Suenaga, K. Furumoto, K. Fukunaga, K. Nakao, Gas–liquid interfacial area, bubble size and liquid-phase mass transfer coefficient in a three-phase external loop airlift bubble column, Chemical and Biochemical Engineering Quarterly 21 (2007) 365–372.
[16] S.L. Kiambi, A.M. Duquenne, A. Bascoul, H. Delmas, Measurements of local interfacial area: application of bi-optical fibre technique, Chemical Engineering Science 56 (2001) 6447–6453.
[17] C.C. Fu, L.S. Fan, W.T. Wu, Flow regime transitions in an internal-loop airlift reactor, Chemical Engineering & Technology 30 (2007) 1077–1082.
[18] C. Vial, S. Poncin, G. Wild, N. Midoux, A simple method for regime identification and flow characterisation in bubble columns and airlift reactors, Chemical Engineering and Processing 40 (2001) 135–151.
[19] G. Vazquez, M.A. Cancela, C. Riverol, E. Alvarez, J.M. Navaza, Application of the Danckwerts method in a bubble column – effects of surfactants on mass transfer coefficient and interfacial area, Chemical Engineering Journal 78 (2000) 13–19.
[20] L. Cheng-Shing, H. Shyh-Jye, Local hydrodynamic properties of gas phase in an internal-loop airlift reactor, Chemical Engineering Journal 91 (2003) 3–22.
[21] X.W. Jia, J.P. Wen, W. Feng, Q. Yuan, Local hydrodynamics modeling of a gas–liquid–solid three-phase airlift loop reactor, Industrial & Engineering Chemistry Research 46 (2007) 5210–5220.
[22] T.F. Wang, J.F. Wang, Y. Jin, A CFD-PBM coupled model for gas–liquid flows, AIChE Journal 52 (2006) 125–140.
[23] R. Krishna, A.J. Dreher, M.I. Urseanu, Influence of alcohol addition on gas hold-up in bubble columns: development of a scale up model, International Communications in Heat and Mass Transfer 27 (2000) 465–472.
[24] A. Blazej, A. Kisa, J. Markos, Scale influence on the hydrodynamics of an internal loop airlift reactor, Chemical Engineering and Processing 43 (2004) 1519–1527.
[25] C.O. Vandu, R. Krishna, Influence of scale on the volumetric mass transfer coefficients in bubble columns, Chemical Engineering and Processing 43 (2004) 575–579.
[26] P.M. Wilkinson, A.P. Spek, L.L. Vandierendonck, Design parameters estimation for scale-up of high-pressure bubble-columns, AIChE Journal 38 (1992) 544–554.
[27] K. Muthukumar, M. Velan, Volumetric mass transfer coefficients in an internal loop airlift reactor with low-density particles, Journal of Chemical Technology and Biotechnology 81 (2006) 667–673.
[28] B. Kawalec-Pietrenko, W. Pietrenko, Generation of small bubbles and small bubble-liquid mass transfer in airlift reactors containing highly viscous liquids, Bioprocess Engineering 21 (1999) 89–95.
[29] H. Dhaouadi, S. Poncin, N. Midoux, G. Wild, Gas–liquid mass transfer in an airlift reactor – analytical solution and experimental confirmation, Chemical Engineering and Processing 40 (2001) 129–133.
[30] H. Dhaouadi, S. Poncin, J.M. Hornut, G. Wild, P. Oinas, J. Korpijarvi, Mass transfer in an external-loop airlift reactor: experiments and modeling, Chemical Engineering Science 52 (1997) 3909–3917.
[31] J.P. Wen, P. Na, L. Huang, Y.L. Chen, Local overall volumetric gas–liquid mass transfer coefficients in gas–liquid–solid reversed flow jet loop bioreactor with a non-Newtonian fluid, Biochemical Engineering Journal 5 (2000) 225–229.
[32] G.Q. Li, S.Z. Yang, Z.L. Cai, J.Y. Chen, Mass-transfer and hydrodynamics in an airlift reactor with viscous non-Newtonian fluid, Chinese Journal of Chemical Engineering 3 (1995) 23–31.
[33] W.A. Al-Masry, M. Chetty, On the estimation of effective shear rate in external loop airlift reactors: non-Newtonian fluids, Resources, Conservation and Recycling 18 (1996) 11–24.
[34] C.H. Wei, B. Xie, H.L. Xiao, D.S. Wang, Volumetric mass transfer coefficient of oxygen in an internal loop airlift reactor with a convergence-divergence draft tube, Chemical Engineering & Technology 23 (2000) 597–603.
[35] A. Mandal, G. Kundu, D. Mukherjee, Studies on frictional pressure drop of gas-non-Newtonian two-phase flow in a cocurrent downflow bubble column, Chemical Engineering Science 59 (2004) 3807–3815.
[36] E. Fransolet, M. Crine, P. Marchot, D. Toye, Analysis of gas holdup in bubble columns with non-Newtonian fluid using electrical resistance tomography and dynamic gas disengagement technique, Chemical Engineering Science 60 (2005) 6118–6123.
[37] Y. Chisti, M. Mooyoung, Improve the performance of airlift reactors, Chemical Engineering Progress 89 (1993) 38–45.
[38] A. Fadavi, Y. Chisti, Gas holdup and mixing characteristics of a novel forced circulation loop reactor, Chemical Engineering Journal 131 (2007) 105–111.
[39] T.F. Wang, J.F. Wang, W.G. Yang, Y. Jin, Bubble behavior in gas–liquid–solid three-phase circulating fluidized beds, Chemical Engineering Journal 84 (2001) 397–404.
[40] C.O. Vandu, R. Krishna, Volumetric mass transfer coefficients in slurry bubble columns operating in the churn-turbulent flow regime, Chemical Engineering and Processing 43 (2004) 987–995.
[41] B. Gourich, C. Vial, N. El Azher, M.B. Soulami, M. Ziyad, Influence of hydrodynamics and probe response on oxygen mass transfer measurements in a high aspect ratio bubble column reactor: effect of the coalescence behaviour of the liquid phase, Biochemical Engineering Journal 39 (2008) 1–14.
[42] S.J. Hwang, Y.L. Cheng, Gas holdup and liquid velocity in three-phase internal-loop airlift reactors, Chemical Engineering Science 52 (1997) 3949–3960.
[43] A.A. Kulkami, Lift force on bubbles in a bubble column reactor: experimental analysis, Chemical Engineering Science 63 (2008) 1710–1723.
[44] A. Tomiyama, H. Tamai, I. Zun, S. Hosokawa, Transverse migration of single bubbles in simple shear flows, Chemical Engineering Science 57 (2002) 1849–1858.
[45] R. Schafer, C. Merten, G. Eigenberger, Bubble size distributions in a bubble column reactor under industrial conditions, Experimental Thermal and Fluid Science 26 (2002) 595–604.
[46] N.A. Kazakis, A.A. Mouza, S.V. Paras, Experimental study of bubble formation at metal porous spargers: effect of liquid properties and sparger characteristics on the initial bubble size distribution, Chemical Engineering Journal 137 (2008) 265–281.
[47] A. Fadavi, Y. Chisti, L. Chriastel, Bubble size in a forced circulation loop reactor, Journal of Chemical Technology and Biotechnology 83 (2008) 105–108.
[48] T.F. Wang, J.F. Wang, W.G. Yang, Y. Jin, Experimental study on bubble behavior in gas–liquid–solid three-phase circulating fluidized beds, Powder Technology 137 (2003) 83–90.
[49] R. Krishna, J. Ellenberger, Gas holdup in bubble column reactors operating in the churn-turbulent flow regime, AIChE Journal 42 (1996) 2627–2634.
[50] J. Zahradnik, M. Fialova, M. Ruzicka, J. Drahos, F. Kastanek, N.H. Thomas, Duality of the gas–liquid flow regimes in bubble column reactors, Chemical Engineering Science 52 (1997) 3811–3826.
[51] M. Letzel, A. Stankiewicz, Gas hold-up and mass transfer in gas-lift reactors operated at elevated pressures, Chemical Engineering Science 54 (1999) 5153–5157.
[52] U. Jordan, A. Schumpe, The gas density effect on mass transfer in bubble columns with organic liquids, Chemical Engineering Science 56 (2001) 6267–6272.
[53] D. Stegeman, P.A. Knop, A.J.G. Wijnands, K.R. Westerterp, Interfacial area and gas holdup in a bubble column reactor at elevated pressures, Industrial & Engineering Chemistry Research 35 (1996) 3842–3847.
[54] S. Maalej, B. Benadda, A. Otterbein, Interfacial area and volumetric mass transfer coefficient in a bubble reactor at elevated pressures, Chemical Engineering Science 58 (2003) 2365–2376.
[55] W. Yang, J. Wang, L. Zhou, Y. Jin, Gas–liquid mass transfer behavior in three-phase CFB reactors, Chemical Engineering Science 54 (1999) 5523–5528.
[56] C.O. Vandu, K. Koop, R. Krishna, Volumetric mass transfer coefficient in a slurry bubble column operating in the heterogeneous flow regime, Chemical Engineering Science 59 (2004) 5417–5423.